Determination of surface convective heat transfer coefficients by CFD

Adam Neale[1]
Dominique Derome[1], Bert Blocken[2] and Jan Carmeliet[2,3]

1) Building Envelope Performance Laboratory, Dep. of Building, Civil and Environmental Engineering, Concordia University, 1455 de Maisonneuve blvd West, Montreal, Qc, H3G 1M8, corresponding author e-mail: aj_neale@encs.concordia.ca

2) Building Physics and Systems, Technische Universiteit Eindhoven, P.O. box 513, 5600 MB Eindhoven, The Netherlands

3) Laboratory of Building Physics, Department of Civil Engineering, Katholieke Universiteit Leuven, Kasteelpark Arenberg 40, 3001 Heverlee, Belgium

ABSTRACT

Heat and vapour convective surface coefficients are required in practically all heat and vapour transport calculations. In building envelope research, such coefficients are often assumed constants for a set of conditions. Heat transfer surface coefficients are often determined using empirical correlations based on measurements of different geometry and flows. Vapour transfer surface coefficients have been measured for some specific conditions, but more often, they are determined with the Chilton-Colburn analogy using known heat transfer coefficients. This analogy breaks down when radiation and sources of heat and moisture are included. Experiments have reported differences up to 300%.

In this paper, the heat transfer process in the boundary layer is examined using Computational Fluid Dynamics (CFD) for laminar and turbulent air flows. The feasibility and accuracy of using CFD to calculate convective heat transfer coefficients is examined. A grid sensitivity analysis is performed for the CFD solutions, and Richardson Extrapolation is used to determine the grid independent solutions for the convective heat transfer coefficients. The coefficients are validated using empirical, semi-empirical and/or analytical solutions.

CFD is found to be an accurate method of predicting heat transfer for the cases studied in this paper. For the laminar forced convection simulations the convective heat transfer coefficients differed from analytical values by ±0.5%. Results for the turbulent forced convection cases had good agreement with universal law-of-the-wall theory and with correlations from literature. Wall functions used to describe boundary layer heat transfer for the turbulent cases are found to be inaccurate for thermally developing regions.

INTRODUCTION

Heat and vapour convective surface coefficients are required in any heat and mass transport calculations. In building envelope research, such coefficients are often assumed constants for a set of conditions. Heat transfer surface coefficients are often determined using empirical correlations based on measurements of different geometry and flows. Convective heat transfer between a moving fluid and a surface can be defined by the following relationship:

$$q_h = h_c\left(T_s - T_f\right) \tag{1}$$

where q_h is the heat flux (W/m^2), h_c is the convective heat transfer coefficient (W/m^{2}K), T_s is the surface temperature (K), and T_f is the fluid reference temperature (K). Similarly, convective vapour transport can be described by the following equation:

$$q_m = h_{m\phi}\left(p_{vsatS}RH_s - p_{vsatR}RH_{ref}\right) \tag{2}$$

where q_m is the mass flux (kg/m^{2}s), $h_{m\varphi}$ is the convective vapour transfer coefficient (kg/m^{2}sPa), p_{vsatS} is the saturation vapour pressure for the surface temperature (Pa), p_{vsatR} is the saturation vapour pressure for the fluid reference temperature (Pa), RH_s is the surface relative humidity in equilibrium with the fluid (-), and RH_{ref} is the fluid reference relative humidity (-). Values of $h_{m\varphi}$ have been measured for some specific conditions (Tremblay *et al* 2000, Derome *et al* 2003, Nabhani *et al* 2003, etc), but more often, they are determined with the Chilton-Colburn analogy or the Lewis analogy using known heat transfer coefficients. The Lewis analogy relates the convective heat and vapour coefficients using the following relationship:

$$h_m = \frac{h_c}{\rho c_p} \tag{3}$$

where ρ is the fluid density (kg/m^3) and c_p is the specific heat (J/kgK). This analogy breaks down when radiation and sources of heat and moisture are included. Experiments have reported differences up to 300% (Derome *et al* 2003), which would have a significant impact on predictions of heat loss through building envelopes, dew point calculations, and many other heat and vapour related calculations.

The convective heat and vapour coefficients can be predicted through detailed experiments or through computer modelling tools that apply discretization schemes (finite element, control volume, etc) to simplify governing equations that normally would have no analytical solution. Experiments have the advantage of providing results tailored to a specific problem, but in order to properly measure boundary layer data expensive equipment such as a Particle Image Velocimetry (PIV) or Laser-Doppler Anemometry (LDA) is often required. Experiments are also generally time consuming to prepare and results inevitably include errors in accuracy. Computer modelling can be used to predict results, but the model must always be validated with experimental data in order to verify the accuracy of the solution. However, it will be shown that other techniques can be employed to validate computer models that do not rely solely on experimental data. With that in mind, this paper will focus primarily on using computer modelling to determine convective heat transfer coefficients.

The purpose of this paper is to demonstrate the feasibility and accuracy of using a commercial Computational Fluid Dynamics (CFD) software to calculate convective heat transfer coefficients. CFD is a modelling technique that breaks down the governing equations (continuity, momentum and energy) for fluid flow into simpler forms that can be solved using numerical techniques (Blocken 2004). The mathematical resolution of the governing equations is still not fully resolved. CFD must then circumvent this by using models to approximate some components of the flow. There are still no universal rules or guidelines on the appropriateness of different models to be use in different problems. Therefore, any CFD calculation must first be validated.

This paper demonstrates how CFD can be used for the determination of the heat transfer process in the boundary layer for two types of flows encountered in buildings, *i.e.* laminar and turbulent air flows. The commercial CFD code *Fluent* 6.1.22 was used for all simulations. The coefficients are validated using empirical, semi-empirical and/or analytical solutions. A grid sensitivity analysis is performed for the CFD solutions, and Richardson Extrapolation is used to determine the grid independent solutions for the convective heat transfer coefficients. Similarly, the combined heat, air and vapour transport can also be analyzed using CFD when coupled with an external model that calculates vapour transport within a solid material, but such calculations are not reported in this paper due to lack of space.

LAMINAR FLOW CFD SIMULATIONS

Heat transfer in the laminar regime will be simulated with CFD for two cases: 1) parallel flat plates with constant heat flux and 2) parallel flat plates with constant wall temperature. Both cases are illustrated below in Figure 1. The geometry is divided into discrete volumes using a structured grid. The number of cells in the grid impacts the solution, as is demonstrated later in the grid sensitivity analysis section. A typical mesh is shown below in Figure 2.

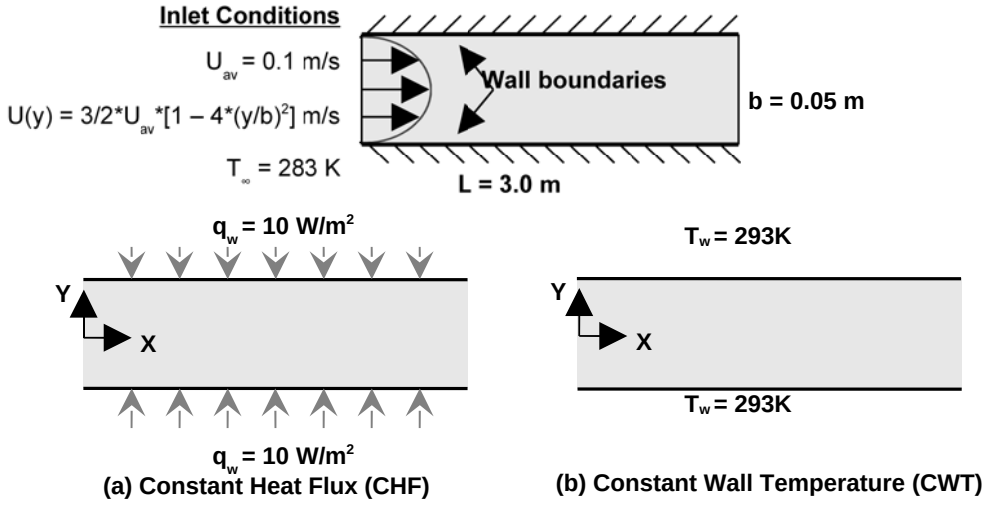

Figure 1. Schematic representation of the two laminar case studies with (a) constant heat flux or (b) constant wall temperature

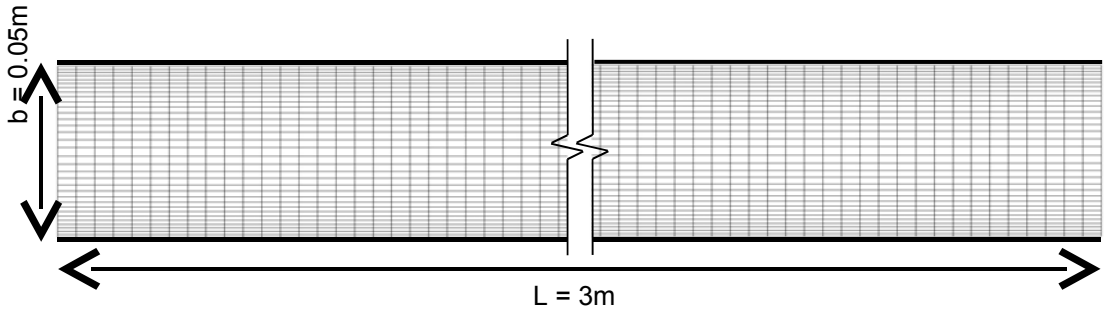

Figure 2. Initial mesh used for the laminar CFD simulations (19,800 elements).

The heat transfer coefficient may be obtained from analytically derived values of the Nusselt number, which should be constant for thermally developed flow between parallel plates. The values differ slightly based upon the heating conditions as follows (Lienhard & Lienhard 2006):

$$Nu_{Dh} = \frac{h_c D_h}{k} = \begin{cases} 7.541 & \textit{for fixed plate temperatures} \\ 8.235 & \textit{for fixed wall heat fluxes} \end{cases} \quad (4)$$

where D_h is the hydraulic diameter (typically twice the distance between parallel plates, m) and k is the thermal conductivity of air (W/mK). The appropriate parameters may then be input to yield the following analytical values for h_c:

$$h_c = \frac{Nu_{Dh} k}{D_h} = \begin{cases} 1.825 & \textit{for fixed plate temperatures} \\ 1.993 & \textit{for fixed wall heat fluxes} \end{cases} \text{ W/m}^2\text{K} \quad (5)$$

Reference Temperature

The equation for convective heat transfer requires a fluid reference temperature, previously designated T_f in Equation 1. The actual value used for T_f depends largely upon the geometry used in the problem. Correlations that describe convective heat transfer coefficients, such as the ones shown in Equation 4, are formulated for one specific reference temperature. An improperly assigned reference temperature can yield a significant error, as will be shown in the laminar case studies presented. Three reference temperatures are used in a comparison exercise to show the effects on the calculation of h_c: a constant reference temperature T_{ref} (as used in Fluent to report h_c values), the centreline temperature T_c (taken at y=0 on Figure 1), and a bulk temperature T_b which is defined as (Lienhard & Lienhard 2006):

$$T_b = \frac{\sum_{i=1}^{n}(u_i b_i T_i)}{U_{av} b} \quad (6)$$

where u_i is the velocity of in the centre of a control volume (CV) (m/s), *i.e.* one cell of the mesh, b_i is the height of the CV (m), T_i the temperature in the CV (K), U_{av} is the velocity averaged over the height (m/s) and b is the height of the domain (m).

The solution procedure to determine the convective heat transfer coefficients for the three reference temperatures is shown below in Table 1. By substituting the known boundary conditions (either the constant heat flux q_w or the constant wall temperature T_w) and the data from the CFD simulation into Equation 7, the convective heat transfer coefficients can be calculated for each point along the length of the plates.

LAMINAR CFD SIMULATION RESULTS

The convective heat transfer coefficients for the constant heat flux case are presented in Figure 3. The results indicate that the temperature value used to describe the fluid (T_f from Equation 1) can have a significant effect on the result. The chosen reference temperature must match the one used in the derivation of the equation or correlation used for comparison. The reported values in *Fluent* are calculated based on a user specified constant reference value, which results in non-constant convective coefficients after thermally developed flow (Fluent Inc. 2003). Correlations that were developed using any other fluid temperature as a reference will not match the results from *Fluent*. Therefore, care must be taken on which values are used when reporting information from *Fluent*.

The convective coefficients calculated from the centerline temperatures are more realistic and follow the expected trend, but they under-predict the h_c values by about 20% for the CHF solution and by about 24% for the CWT solution.

Table 1. Convective heat transfer coefficient solution parameters

	CHF – Case (a)	**CWT – Case (b)**
$q_w(x)$	q_w = 10 W/m^2	$q_w(x)$ → From *Fluent*
$T_w(x)$	$T_W(x)$ → From *Fluent*	T_w = 293 K

$T_f(x)$	$h_c(x) = \frac{q_w(x)}{T_w(x) - T_f(x)}$ (7)	
$T_f(x) = T_{ref}$ = 283 K (Constant value specified in Fluent (Fluent Inc. 2003))	$h_{cRef}(x) = \frac{10}{T_w(x) - 283}$	$h_{cRef}(x) = \frac{q_w(x)}{293 - 283}$
$T_f(x) = T_c(x)$ (Horizontal temperature profile at the center of the flow (y = 0))	$h_{cc}(x) = \frac{10}{T_w(x) - T_c(x)}$	$h_{cc}(x) = \frac{q_w(x)}{293 - T_c(x)}$
$T_f(x) = T_b(x)$ (Bulk Temperature calculated at different x positions from the Fluent Data)	$h_{cb}(x) = \frac{10}{T_w(x) - T_b(x)}$	$h_{cb}(x) = \frac{q_w(x)}{293 - T_b(x)}$

The bulk temperature yielded the best solution for the convective heat transfer coefficient, resulting in an error margin of less than 0.5% for both cases (after thermal development). Since the bulk temperature calculation, the wall temperature and the wall heat flux are all dependent on the grid used, a grid sensitivity and discretization error analysis was performed to determine what the grid independent solution would be.

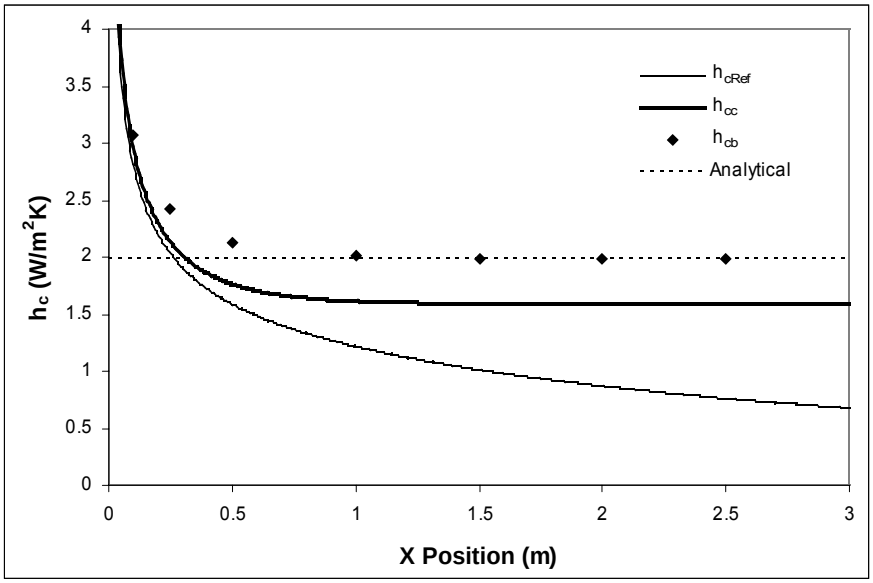

Figure 3. Convective heat transfer coefficients for constant wall heat flux

Grid Sensitivity Analysis

The determination of a mesh for the CFD calculations is not a trivial task. A mesh that is too coarse will result in large errors; an overly fine mesh will be costly in computing time. To demonstrate the impact of the mesh size on the calculation results, any CFD simulation should be accompanied by a grid sensitivity analysis. One such analysis is presented here.

For the purposes of the grid sensitivity analysis, the convective heat transfer coefficients are calculated and compared for different grid densities at x = 2.5 m. The process was repeated for both the CHF and CWT cases to compare the grid dependency for the two different boundary conditions. Only the coefficients calculated from the bulk temperature are part of this comparison.

Table 2. Mesh dimensions

	φ_h (80400)	φ_{2h} (19800)*	φ_{4h} (5100)	φ_{8h} (1200)	φ_{16h} (300)
Number of cells in the Y Direction	67	33	17	8	4
Number of cells in the X Direction	1200	600	300	150	75
Smallest cell height (m)	4.202E-04	8.749E-04	1.775E-03	3.948E-03	9.147E-03
Smallest cell width (m)	0.0025	0.005	0.01	0.02	0.04
Total number of cells	80400	19800	5100	1200	300

*** Original mesh**

The initial grid used for the simulations had a total of 19,800 cells. It was decided to proceed with several coarser grids and one finer mesh. The details of the different meshes are presented in Table 2. The notation ϕ_h is adopted to describe the solution for the finest mesh. The subsequent meshes are all notated with respect to the finest mesh. The next grid size has cell dimensions doubled in both directions, hence the notation ϕ_{2h}. It can be shown (Ferziger & Peric 1997) that the discretization error of a grid is approximately:

$$\varepsilon_h^d \approx \frac{\phi_h - \phi_{2h}}{2^a - 1} \tag{8}$$

where a is the order of the scheme and is given by

$$a = \frac{\log\left(\frac{\phi_{2h} - \phi_{4h}}{\phi_h - \phi_{2h}}\right)}{\log(2)} \quad (9)$$

In both equations the "2" refers to the increase in dimensions of the mesh. From Equation 9, it follows that a minimum of three meshes are required to determine the discretization error. In order to prevent a calculation error from the logarithm of a negative number, the three solutions must be monotonically converging.

The theory of Richardson Extrapolation states that the solution from the finest mesh can be added to the discretization error found from Equation 8 to attain an approximate grid independent solution. In equation form this can be stated as:

$$\Phi = \phi_h + \varepsilon_h^d \quad (10)$$

The convective heat transfer coefficients for the constant heat flux case are plotted below in Figure 4 and the results from the grid sensitivity analysis are shown in Table 3.

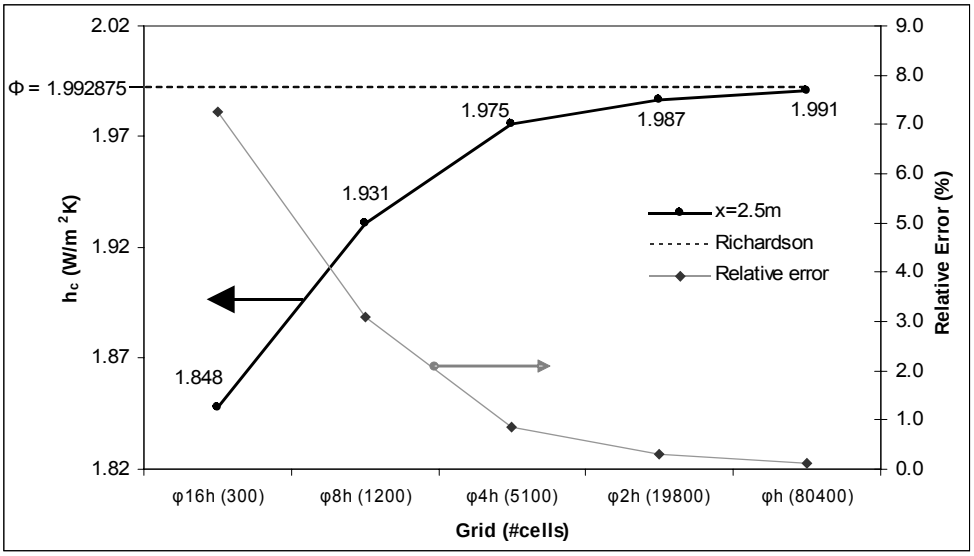

Figure 4. Grid convergence of the heat transfer coefficient for constant heat flux and relative error compared with Richardson solution

Table 3. Discretization error and Richardson Extrapolation Results

	Order of the scheme a	Discretization Error ε_h^d (W/m²K)	Finest mesh solution ϕ_h (W/m²K)	Richardson Solution Φ (W/m²K)	Analytical solution h_c (W/m²K)
CHF	1.460	2.297×10^{-3}	1.990578	1.992875	1.992875
CWT	1.858	1.001×10^{-3}	1.824089	1.825090	1.824922

TURBULENT FLOW CFD SIMULATIONS

The second type of air flow to be studied is turbulent flow on surfaces, such as encountered on exterior claddings subjected to wind. In the interest of validating the different turbulent models within *Fluent* for the purpose of calculating the convective heat transfer coefficients, it was necessary to obtain experimental data to use as a basis for comparison. While experiments have been performed in this area, it is often difficult to establish whether the simulation truly matches all of the experimental parameters. However, one area of research that has been focused on extensively in the past is the universal "law-of-the-wall" that describes turbulent boundary layer flow. Through analytical derivations of equations and experimental data fitting, the boundary layer velocity profile (and temperature profile, if applicable) has been subdivided into three regions: the laminar sublayer, the buffer region, and log-law region (Chen & Jaw 1998, Blocken 2004). Semi-empirical relationships

have been developed for the laminar sublayer and log-law regions, and empirical equations exist for the buffer region as well (e.g. Spalding 1961). The (semi-)empirical equations will be used to validate the simulation results from *Fluent*.

Near-wall modelling

Boundary layer (BL) velocity and temperature profiles are generally described using dimensionless parameters. Before the BL regions can be discussed in proper detail, some dimensionless terms must be introduced:

$$y^+ \equiv \frac{yu^*}{\nu} \qquad \text{where} \quad u^* \equiv \sqrt{\frac{\tau_w}{\rho}}, \qquad \text{and} \qquad \tau_w \equiv \mu \left.\frac{\partial U}{\partial y}\right|_{y=0} \tag{11}$$

where y^+ is the dimensionless distance from the wall (-), y is the distance from the wall (m), ν is the kinematic viscosity (m^2/s), u^* is the friction velocity (m/s), τ_w is the wall shear stress (Pa), ρ is the fluid density (kg/m^3), U is the mean fluid velocity along the wall (m/s), and μ is the dynamic viscosity (kg/m-s). The velocity can be described in a dimensionless form as a function of the mean fluid velocity and the friction velocity:

$$u^+ \equiv \frac{U}{u^*} \tag{12}$$

For cases with heat transfer, the dimensionless temperature may be calculated using the following equation:

$$T^+ \equiv \frac{T_w - T}{T^*} \qquad \text{where} \quad T^* \equiv \frac{\alpha q_w}{k u^*} \tag{13}$$

where T_w is the wall temperature at a certain point (K), T is the fluid temperature (K), α is the thermal diffusivity (m^2/s), q_w is the wall heat flux (W/m^2) and k is the thermal conductivity (W/mK).

There are two common near-wall modelling techniques employed in CFD: Low-Reynolds-number modelling and Wall function theory.

Low-Reynolds-number modelling (Low-Re)

If the boundary layer is meshed sufficiently fine so that the first cell is placed entirely in the laminar sublayer of the BL, the approach used is generally referred to as Low-Re Modelling. In Low-Re modelling, the governing equations of fluid flow are solved in all regions of the BL. It is more time consuming but generally more accurate than the wall-function approach. In dimensionless units, the height of the first cell is generally taken to be approximately $y^+ = 1$, though the laminar sublayer is valid up to $y^+ < 5$ (Blocken 2004). In the range of $5 < y^+ < 30$ there exists a buffer region between the laminar sublayer and the log-law region of the boundary layer. It is generally not advisable to have meshes where the first cell lies within the buffer region, though often it is unavoidable in CFD. For meshes where the first cell is located at $y^+ > 30$, wall function theory may be applied.

Wall function theory

Fluid flow over a smooth flat plate is referred to as the simplest case for analytical fluid dynamics (Schetz 1993). There has been a significant amount of work done in experiments for boundary layer flow evaluation (summarized in Bejan 1984, Schlichting 1987, Schetz 1993, Chen & Jaw 1998, etc). That work was subsequently transformed into the *wall function* concept (e.g. Spalding 1961). Wall functions allow CFD models to interpret behaviour near a wall without the need for a very fine mesh that discretises the generally quite thin laminar sublayer at the surface of the wall. The wall function equations are based on an analytical solution of the transport equations in combination with experimental data fitting. The result is a reduction in computation time and a relatively accurate representation of what happens within the BL, at least under the conditions for which the wall functions were derived. Wall functions are recommended for cases where the domain is complex or so large that it would require an extremely elaborate mesh leading to a long computation time. On the other hand, wall functions may cease to be valid in complex situations. Nevertheless, they are often used – even when not valid – for complex calculations, which can be responsible for considerable errors in near-wall flow and the related convective heat transfer coefficients (Blocken 2004).

Wall functions are generally described as having two regions: the laminar sublayer and the log-law layer. It is commonly accepted in CFD that the laminar sublayer is said to be valid in the region where $y^+ <$ (5 to 10) (Chen & Jaw 1998). The equations for the dimensionless velocity and temperature within this region are (Fluent Inc. 2003):

$$u^+ = y^+ \tag{14}$$

$$T^+ = \mathrm{Pr}\, y^+ \tag{15}$$

where Pr is the Prandtl number ($Pr = \nu/\alpha$). The region above the laminar sublayer ($y^+ > 30$) is the log-law layer, which is generally described in the form of (Fluent Inc. 2003):

$$u^+ = 2.5 \ln y^+ + 5.45 \tag{16}$$

$$T^+ = \mathrm{Pr}_t \left[\frac{1}{\kappa} \ln(Ey^+) + P \right] \tag{17}$$

where Pr_t is the turbulent Prandtl number (= 0.85 for air), E is an experimentally determined constant (= 9.793), and P is a function of the Prandtl and turbulent Prandtl numbers.

Spalding (1961) suggests an equation that will cover the entire y^+ range of values for the dimensionless velocity $u+$ (including the buffer region):

$$y^+ = u^+ + A\left[\exp Bu^+ - 1 - Bu^+ - \frac{1}{2}(Bu^+)^2 - \frac{1}{6}(Bu^+)^3 - \frac{1}{24}(Bu^+)^4 \right] \tag{18}$$

where $A=0.1108$ and $B=0.4$. The equations for the dimensionless velocity and temperature are illustrated in Figure 5.

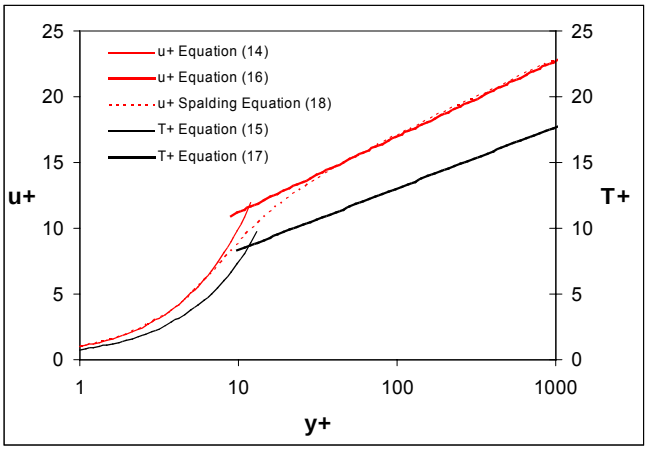

Figure 5. Wall function dimensionless velocity and temperature distributions

Heat transfer in turbulent flow

Convective heat transfer coefficients are generally expressed in the form of dimensionless correlations that are based on experimental data. There are a number of works in literature that summarize the numerous correlations that exist for different types of flows (e.g. Bejan 1984, Saelens 2002, Lienhard & Lienhard 2006). For the purpose of this paper, two correlations were selected from Lienhard & Lienhard (2006) that correspond to the geometry and flow conditions for the forced convection cases that were simulated. They are given by Equations 19 and 20 below.

$$St_x = \frac{C_{fx}/2}{1 + 12.8\left(\mathrm{Pr}^{0.68} - 1\right)\sqrt{C_{fx}/2}}; \qquad Pr > 0.5 \tag{19}$$

$$Nu_x = 0.032\, \mathrm{Re}_x^{0.8}\, \mathrm{Pr}^{0.43} \tag{20}$$

Reynold's Number: $\mathrm{Re}_x \equiv \dfrac{\rho U_\infty x}{\mu}$ *Prandtl Number:* $\mathrm{Pr} \equiv \dfrac{\nu}{\alpha}$

Stanton Number: $St \equiv \dfrac{h_c}{\rho c_p U_\infty}$ *Nusselt Number:* $Nu_x \equiv \dfrac{h_c x}{k}$

Skin Friction Coefficient: $C_{fx} = \frac{0.455}{[\ln(0.06\,\mathrm{Re}_x)]^2}$ (White 1969)

TURBULENT FORCED CONVECTION SIMULATIONS

The domain used to represent fluid flow over a flat plate is shown in Figure 6. The boundary condition (BC) for the top of the domain was chosen to be a symmetry condition in order to reduce the computation time of the simulation. If a pressure outlet BC is chosen instead of symmetry it can lead to convergence problems when modelling turbulence. The height of the domain was selected to be high enough to reduce the influence of the symmetry condition on the boundary layer.

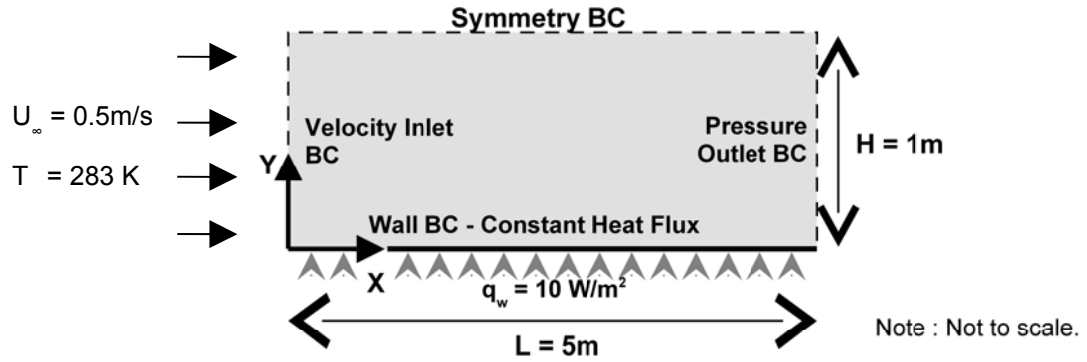

Figure 6. Computational domain and boundary conditions (BC)

As explained previously, the Low-Re modelling approach recommends that the first grid cell has a dimensionless height of $y^+ \approx 1$, which means that it is submerged in the laminar sublayer. (Fluent Inc. 2003). For simulations with Wall Functions (WF), a y^+ between 30 and 60 is recommended. The y^+ value is based on the flow conditions at the surface and therefore requires an iterative procedure to properly size the first cell. After a number of grid adjustments the mesh fulfilled the requirements for Low-Re modelling, and is shown below in Figure 7 with the wall function mesh. An exponential relationship was used to mesh the vertical direction and a uniform spacing was used for the horizontal direction. The grid dimensions are shown in Table 4.

Table 4. Grid parameters and dimensions – turbulent forced convection cases

Grid	#Cells in X-direction	#Cells in Y-direction	Smallest Cell Width	Smallest Cell Height	Total number of cells
Low-Re	500	100	0.01 m	1.285×10^{-3} m	50000
WF	100	13	0.03 m	4.653×10^{-2} m	1300

Note that the grids for the Low-Re modelling and wall function cases can have the same spacing near the symmetry boundary, since the boundary layer resolution is not affected by the top region of the domain.

The simulations were all initialized with a uniform velocity profile of 0.5 m/s. The simulations were iterated until the scaled residuals for all parameters were below 10^{-7}. The outlet velocity profile and turbulence conditions were then used as the new inlet conditions and the simulation was repeated. The thermal conditions were not saved from one simulation to the next, and consequently the flow was always thermally developing from the start of the domain. This procedure was continued until the inlet and outlet velocity profiles were approximately the same, resulting in a fully developed flow profile. By using this procedure the domain of the problem is reduced in length, which significantly decreases computation time. The original uniform velocity profile ensured that the bulk velocity was 0.5 m/s for all cases.

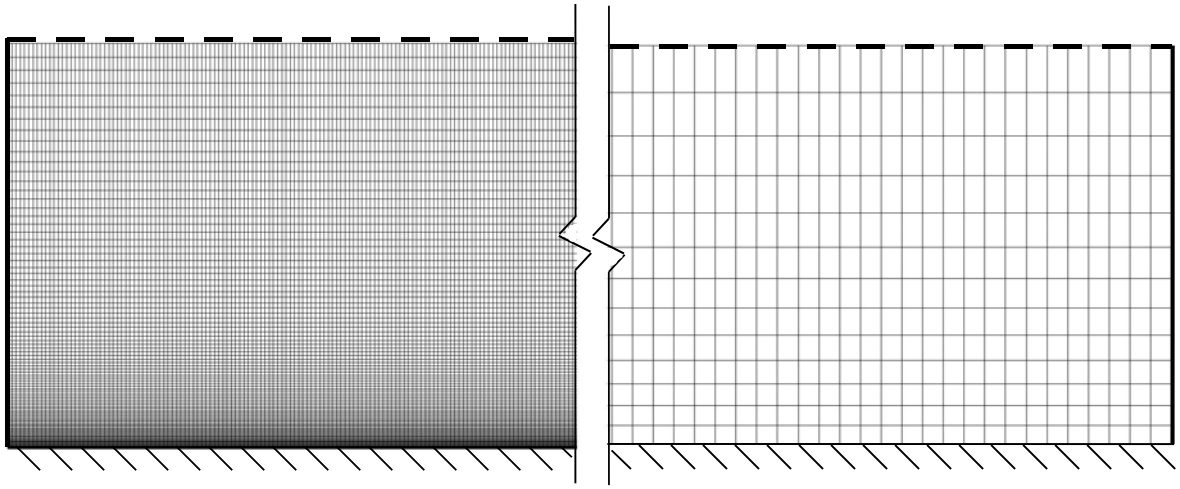

Figure 7. Grids used for low-Reynolds-number modelling (left) and wall functions (right)

SIMULATION RESULTS FOR FORCED CONVECTION

The simulation results are compared at x=4.5m for all cases. Simulations were performed with the following turbulence models with Low-Re Modelling:

1) *Spalart-Allmaras Model*
2) *Standard k-ε Model*
3) *RNG k-ε Model*
4) *Realizable k-ε Model*
5) *Standard k-ω Model*
6) *SST k-ω Model*
7) *Reynold's Stress Model (RSM)*

Simulations were performed with the following models with Wall Functions (WF):

1) *Standard k-ε Model*
2) *Standard k-ω Model*

Note that the *Standard k-ω Model* will automatically interpret whether Low-Re or WF will be used based on the y^+ of the first cell. The default settings for each model were used for all cases unless otherwise specified.

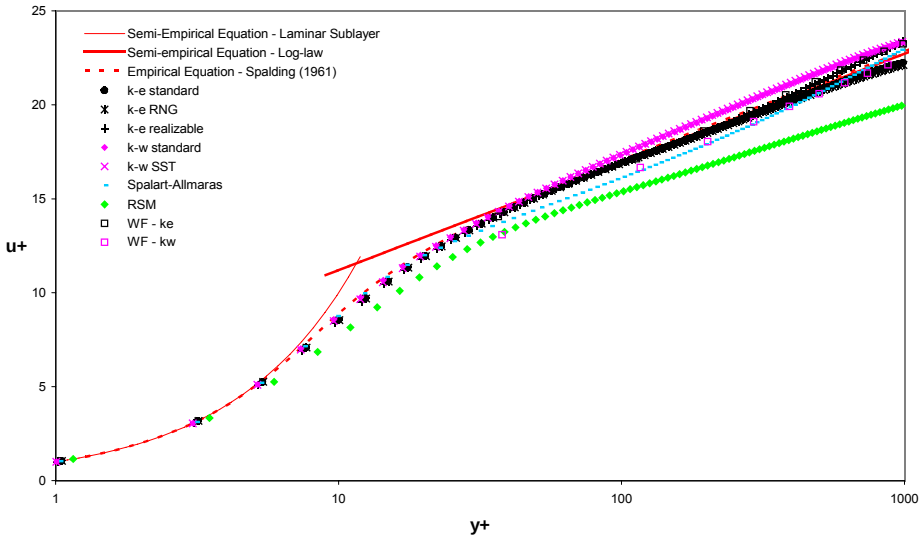

Figure 8. Dimensionless velocity profile results for the turbulent simulations

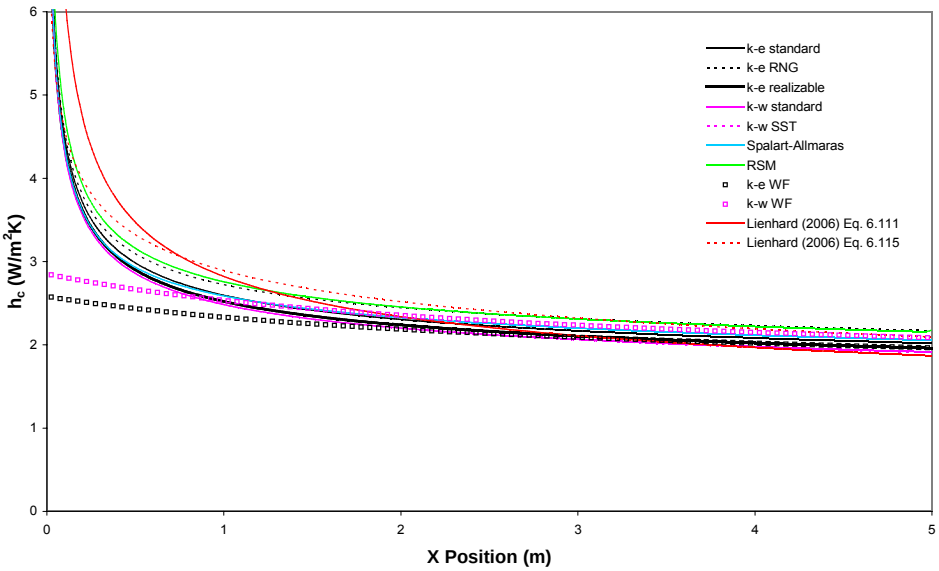

Figure 9. Convective heat transfer coefficient results for the turbulent simulations

TURBULENT FORCED CONVECTION RESULTS SUMMARY

The velocity profiles shown in Figure 8 indicate a good agreement with the "universal" law-of-the-wall relationships and the "universal" Spalding curve, which were both developed based on experimental data. The laminar sublayer and the log-law region are well defined for all of the turbulence models, though some models (RSM) tend to under predict the velocity near the upper boundary (for large values of y^+). This can be explained by the fact that the law-of-the-wall relationship ceases to be valid beyond a certain point (roughly $y^+ > 500$) (Blocken 2004). Similar results were obtained for the dimensionless temperature profiles.

The correlations for heat transfer are shown in red on Figure 9. The heat transfer coefficients are consistent between the turbulence models and the correlations, including the solutions using wall functions. However, in the thermally developing region (approximately 0m < x < 1m), the wall function solutions differ from the other curves. The result is an important underprediction of heat transfer for cases where there is thermally developing flow. This is due to the fact that the wall function approach is not valid under these conditions.

CONCLUSIONS

Computational Fluid Dynamics can be used to determine the convective heat transfer coefficients. This paper demonstrated the use of CFD for heat flow in forced laminar and turbulent air flows. This paper also gives a few guidelines on the use of CFD to perform such calculations.

First, a validation exercise was performed by comparing the computed convective heat transfer coefficients (h_c) for laminar air flow between parallel plates by Computational Fluid Dynamics to analytical solutions. The CFD simulations were performed for constant wall temperature and constant heat flux conditions. The importance of a correct reference temperature was confirmed. The CFD results showed a good agreement with the analytical solutions, indicating a proper performance of the CFD code, at least for the cases studied.

A grid sensitivity analysis was performed on the mesh for both laminar cases. The discretization error for h_c was calculated at a given location on the plate and Richardson extrapolation was used to compute the grid independent solution. The resulting h_c values had good agreement with analytical values from literature. The percentage error between the analytical and the grid independent solutions for h_c is on the order of 10^{-2} %.

The turbulent models within *Fluent* were validated using universal "law-of-the-wall" theory. Semi-empirical relationships developed using experimental data and analytical theory were used to validate the simulation results for forced convection over a smooth flat plate. The results indicate a

good agreement between (semi-)empirical equations and simulation boundary layer velocity and temperature profiles for all of the turbulence models studied.

The heat transfer coefficients calculated from the turbulent forced convection simulations are consistent for all of the turbulent models studied, and also coincide closely with selected correlations from literature. The results for simulations with wall functions indicate that the heat transfer coefficients calculated in the thermally developing region of the domain are not consistent with the Low-Re simulation results or with the correlations. It is concluded that the wall functions are not valid for thermally developing regions.

The laminar and turbulent convective heat transfer models for CFD have been shown to calculate the convective heat transfer coefficients with good agreement with experimental and analytical values. As a result, the CFD models can be used with confidence for cases similar to the ones described here. It is also possible to calculate vapour convective transfer coefficients, although not reported in this paper, by coupling to the CFD model an external vapour transport model developed by the authors, for the purpose of calculating combined heat and vapour transport for laminar air flow over porous materials, such as wood. Once the heat and vapour transfer model in Fluent are validated, the calculated heat and vapour convective transfer coefficients can be used by calculation models of building envelope performance.

REFERENCES

1) Bejan, A., "Convection Heat Transfer," John Wiley & Sons, Inc., 1984.
2) Blocken, B., "Wind-driven rain on buildings," Ph.D. thesis, Leuven: K.U.Leuven., 2004.
3) Chen, C.-J., Jaw, S.-Y., "Fundamentals of Turbulence Modeling," Taylor & Francis, 1998.
4) Derome, D., Fortin, Y., Fazio, P., "Modeling of moisture behavior of wood planks in nonvented flat roofs." J. of Architectural Eng., ASCE, 9:26-40, March 2003.
5) Ferziger, J.H., Perić, M. "Computational Methods for Fluid Dynamics." Springer, 3rd Edition, 58-60, 2002.
6) Fluent 6.1 User's Guide, 2003.
7) Lienhard IV, J.H., Lienhard V, J.H. "A Heat Transfer Textbook", Phlogiston Press, 2006.
8) Nabhani, M., Tremblay, C., Fortin, Y., "Experimental determination of convective heat and mass transfer coefficients during wood drying." 8th Intl. IUFRO Wood Drying Conference, 225-230, 2003.
9) Saelens, D., "Energy performance assessment of single story multiple-skin facades," Ph.D. dissertation, Leuven: K.U.Leuven, 2002.
10) Schetz, J.A., "Boundary Layer Analysis." Prentice Hall, 1993.
11) Schlichting, H., "Boundary-Layer Theory," McGraw-Hill, 7th Edition, 1987.
12) Spalding, D.B., "A single formula for the law of the wall," J. Appl. Mech., Vol 28, 1961, pp. 455-457.
13) Tremblay, C., Cloutier, A., Fortin, Y., "Experimental determination of the convective heat and mass transfer coefficients for wood drying." Wood Science and Technology 34, 253-276, 2000.
14) White, F.M., "A new integral method for analyzing the turbulent boundary layer with arbitrary pressure gradient," J. Basic Engr., 91: 371-378, 1969.